Chemical Science

RSC Publishing

EDGE ARTICLE

View Article Online
View Journal

On the role of anionic ligands in the site-selectivity of oxidative C–H functionalization reactions of arenes†

Cite this: DOI: 10.1039/c3sc00017f

Italo A. Sanhueza,[a] Anna M. Wagner,[b] Melanie S. Sanford*[b] and Franziska Schoenebeck*[a]

The replacement of an acetate ligand for carbonate leads to a reversal in site-selectivity in the Pd-mediated C–H oxidative coupling of benzo[*h*]quinoline with 1,3-dimethoxybenzene. This report describes Density Functional Theory studies designed to elucidate the origin of this selectivity change. These studies focused on two key mechanistic steps: C–H activation and C–C bond-forming reductive elimination. We considered monometallic and bimetallic reaction pathways for acetate and carbonate conditions. The favored C–H activation pathway proceeds *via* a concerted metalation deprotonation (CMD) mechanism, independent of the nature of anionic ligand (acetate *versus* carbonate). The predicted selectivity is *ortho*/*para* for the C–H activation for both the acetate and carbonate-ligated Pd complexes. Further, we determined that the reductive elimination step is greatly facilitated by the coordination of benzoquinone (by $\Delta\Delta G^{\ddagger} \sim 20$ kcal mol^{-1}) and is predicted to be *meta–meta* selective with both anionic ligands. Overall, the DFT studies indicate that the anionic ligand does not induce a mechanism change at the elementary steps, and the predicted selectivity at all steps is equivalent for carbonate and acetate, no matter whether a dinuclear or mononuclear pathway is considered. These studies lead us to propose that the role of the anionic ligand is to control which step of the mechanism is overall selectivity-determining. This proposal has been tested experimentally using appropriately designed experiments. Notably, the insoluble base MgO as an acid trap under acetate conditions (with the aim of making the C–H insertion step less reversible), gave rise to predominant *ortho*/*para* selectivity in the presence of acetate, in analogy to the results previously seen under carbonate conditions.

Received 3rd January 2013
Accepted 22nd April 2013

DOI: 10.1039/c3sc00017f

www.rsc.org/chemicalscience

Introduction

Direct functionalization of C–H bonds *via* palladium catalysis has become an increasingly attractive strategy for the synthesis and derivatization of natural products and pharmaceutically relevant building blocks.[1] Despite vast progress in this field over the past 10 years, several key challenges remain. In particular, the control of site-selectivity in Pd-catalyzed C–H functionalization requires significant further development, in both reaction discovery and mechanistic understanding.[2,3] The most frequently applied approach to control site-selectivity is the use of substrates that contain *ortho*-directing groups, which pre-organize the Pd-catalyst through coordination.[1,4] In marked contrast, only a few examples of reactions where site-selectivity is controlled by catalyst structure and/or reaction conditions have been reported.[2,3] Furthermore, the mechanistic origins of the observed selectivities generally remain poorly understood. In this context, Sanford and co-workers have recently demonstrated that site-selectivity in Pd-mediated oxidative coupling reactions is highly dependent on the anionic ligand associated with the Pd-center.[5] When performing stoichiometric experiments with cyclopalladated [BzqPd(II)X]$_2$ (Bzq = benzo[*h*]quinoline) and a large excess of 1,3-dimethoxybenzene (300 equiv.) in the presence of 4 equiv. of DMSO, and 1 equiv. of benzoquinone (BQ) at 150 °C (see Scheme 1), it was discovered that the use of acetate as the anion (X) resulted in a 16 : 1 preference for the *meta–meta* oxidative coupling product **A**. In contrast,

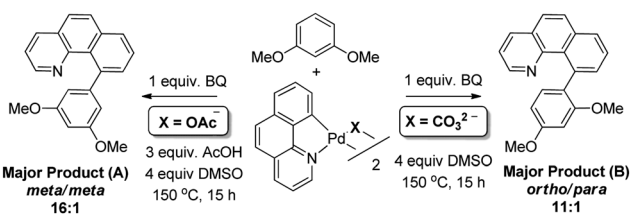

Scheme 1 Anion-dependent selectivity in oxidative coupling.

[a]*Laboratory for Organic Chemistry, ETH Zürich, Wolfgang-Pauli-Strasse 10, 8093 Zürich, Switzerland. E-mail: schoenebeck@org.chem.ethz.ch; Web: http://www.schoenebeck.ethz.ch/*

[b]*Department of Chemistry, University of Michigan, 930 North University Avenue, Ann Arbor, Michigan 48109, USA. E-mail: mssanfor@umich.edu; Web: http://www.umich.edu/~mssgroup/*

† Electronic supplementary information (ESI) available: Computational details, absolute energies, thermochemistry, and Cartesian coordinates of all calculated structures; full ref. 6 and experimental details. See DOI: 10.1039/c3sc00017f

substitution of acetate for carbonate gave high selectivity for the *ortho*/*para* coupling product **B** (11 : 1 ratio). The origin of this selectivity reversal is currently not understood,[5] and the rational design of new, more selective reactions as well as the application of these transformations to wider classes of substrates will require a detailed understanding of the mechanistic details and factors controlling selectivity. We herein report Density Functional Theory[6] studies designed to elucidate the origin of selectivity in this Pd-mediated oxidative coupling between benzo[*h*]quinoline and 1,3-dimethoxybenzene as a function of anionic ligand (Scheme 1). We also demonstrate the design and implementation of experiments to confirm our computationally derived conclusions.

Results and discussion

Mechanistic studies suggest that this transformation proceeds *via* the pathway illustrated in Scheme 2. The two key steps with respect to site-selectivity are (i) the C–H activation of aryl-H (Step 1) and (ii) C–C bond-forming reductive elimination (Step 3). Importantly, the reductive elimination step is greatly facilitated by the presence of benzoquinone (BQ).[5,7] Detailed experimental mechanistic studies suggest that this is due to coordination of the BQ to a Pd-intermediate (Step 2), and this is supported by recent computational studies of an oxidative Heck reaction.[8] In addition to facilitating the reductive elimination, the concentration of benzoquinone can also affect site-selectivity under some conditions. For example, when acetate is the anionic ligand, a high concentration of BQ (~10 equiv.) gives rise to much lower selectivity (A : B ~ 1 : 1). Interestingly, and in marked contrast, with carbonate as the counterion, the A/B selectivity is independent of BQ concentration.[5]

On the basis of this general mechanism, the changes in selectivity as a function of ligand (acetate *vs.* carbonate) could potentially be due to: (1) a change in the mechanism of the C–H activation step upon changing the anionic ligand at Pd, (2) a change in the site-selectivity of the C–H activation step (with no change in the overall mechanism), (3) a change in the selectivity of the quinone-promoted reductive elimination step, or (4) a change in the selectivity-determining step of the overall reaction as a function of ligand. It is important to note that there are several unknown variables in this sequence. Most importantly, the coordination environment at palladium in the various intermediates and transition states is unknown. Benzoquinone could coordinate to several possible intermediates;[5,7] furthermore, there is no information available on the precise nature of ligands (L).

Given the large number of possible intermediates, we chose the following strategy to explore the anion effect on selectivity in the oxidative coupling of benzo[*h*]quinoline and 1,3-dimethoxybenzene. First, we calculated the C–H activation transition state preference as a function of anion (acetate *versus* carbonate) and mechanism. Then we independently studied the BQ-promoted reductive elimination (Steps 2/3) and calculated the transition states and relevant intermediates prior to elimination for the different anionic ligands and for a number of potential ligation states. These calculations provide critical insights into the origins of selectivity reversal as a function of anionic ligand. The insights gleaned from the DFT studies were then subsequently tested experimentally.

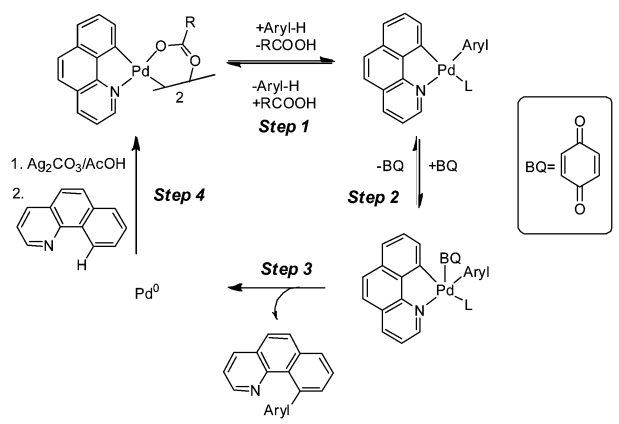

Scheme 2 Proposed mechanism of C–H functionalization.[5]

Computational details and choice of system for calculations

All calculations were performed with Gaussian09,[6] unless otherwise stated. The structures presented in the main manuscript were optimized in the gas-phase using ωB97XD[9]/6-31G(d,p) and LANL2DZ[10] (for Pd and Na). Frequency calculations were performed on all gas-phase optimized geometries to verify the nature of all stationary points as either minima or transition states. Single point energies were then calculated with M06L[11] with SDD[12] for Pd (and Na) and 6-31++G(d,p) or def2-TZVPP. The solvation model COSMO-RS[13] was employed to account for solvation. The standard state was converted to 1 M in solution (+1.89 kcal mol^{-1}).

Dispersive effects are expected to be particularly relevant in considerations of monomeric *versus* dimeric pathways and the Pd···BQ interaction (but see later discussion for potential overestimation of these effects). Potential inaccuracies in the analyses of mono *versus* dimeric pathways due to the basis set superposition error (BSSE)[14] may also arise; we therefore also considered alternative methods for energy calculations (*e.g.* PBE0-D3, PBE0) or basis set (def2-TZVPP) in addition to the above computational approach. The results are discussed in the main manuscript.

We undertook the majority of preliminary conformational searches with ωB97XD/3-21G optimization, with later refinement at ωB97XD/6-31G(d,p) and M06L treatment. A method and basis set comparison study for the *ortho*/*para* pathway (for acetate) from Fig. 2 (presented in the ESI†) suggest that this was adequate. The results of this study are summarized in the ESI (page S6†) and compare the basis sets 6-31+G(d), 6-31G(d,p) and 3-21G with LANL2DZ (for Pd) for geometry optimizations with the methods ωB97XD or B3LYP[15] as well as the single point energy methods: PBE0, PBE0-D3 (ref. 16) and M06L with 6-31++G(d,p), SDD (Pd) basis set or def2-TZVPP.[11,24] This study showed that there is barely any dependency of the activation barriers of the individual steps on the basis set.

In order for the solvation model, COSMO-RS, to be applicable, the experimental conditions need to be homogeneous, so that the effect of solvation on reactivity can be modeled. The original reaction conditions by Sanford *et al.* (see Scheme 1, *i.e.* 300 equiv. of 1,3-dimethoxybenzene and 4 equiv. DMSO) were heterogeneous when carbonate was employed as the anionic ligand. Thus, we initially performed an experimental solvent screen with varying amounts of DMSO (4 to 300 equivalents) to render the reaction homogeneous. The selectivity only changed slightly under the homogeneous reaction conditions (1,3-dimethoxybenzene/DMSO, 300 : 50) and the overall selectivity trend was unaffected (see Table S1–S3, p. S2 in the ESI†). We also determined experimentally that the counter-cation of the carbonate salt (Cs^+ and Na^+ were tested) had no marked effect on the selectivity (see p. S2 in the ESI†).

On the basis of this data, we decided to perform the computational studies using $NaCO_3^-$ or OAc^- as anionic ligands and applying COSMO-RS calculations for the solvent mixture.

Study of step 1: C–H activation as a function of anionic ligand and mechanism. As shown in Scheme 3, there are several potential mechanisms for the C–H activation step including: (a) electrophilic aromatic substitution (S_EAr),[17] (b) concerted metalation deprotonation (CMD)[18] or (c) a Heck-type arylation pathway.[1,4,19–21]

Previous preliminary DFT investigations by the Sanford group suggested against an electrophilic aromatic substitution (S_EAr) mechanism based on a poor correlation of the relative energies of the intermediates with experimental data.[5a] Analogous conclusions have also recently been made in related work by Zhang *et al.*[22] We therefore focused our investigations on mechanisms (b) and (c), *i.e.* the CMD and the Heck type pathways (Scheme 3).

The CMD pathway features a six-membered transition state in which the anionic ligand (acetate or carbonate) participates in a concerted deprotonation of the arene, while Pd inserts into the C–H bond (Scheme 3). Recent studies by Hartwig and coworkers have suggested the potential direct involvement of a cyclopalladated dinuclear Pd complex in the C–H arylation of pyridine *N*-oxide.[23] We therefore calculated CMD C–H activation by the dinuclear and mononuclear Pd(II) complex for both acetate and carbonate and the two possible sites on the arene (*ortho* or *meta* in 1,3-dimethoxybenzene). We applied the following naming convention: $\mathbf{TS_{CMD(m–m)}}$ or $\mathbf{TS_{CMD(o–p)}}$ that would lead to the *meta–meta* product **A** or the *ortho*/*para* product **B**, respectively (see Fig. 1 and Scheme 1).

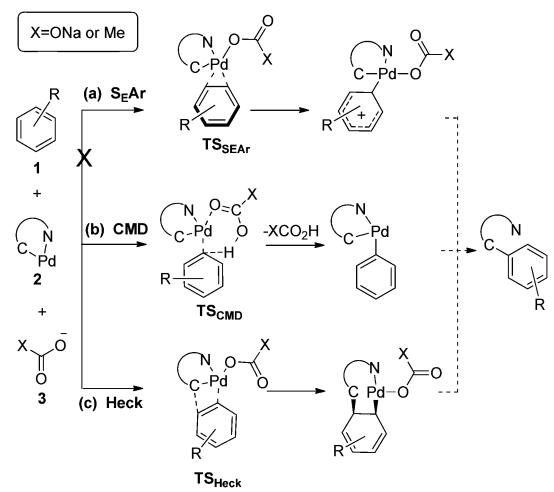

Scheme 3 Mechanistic possibilities for C–H activation.

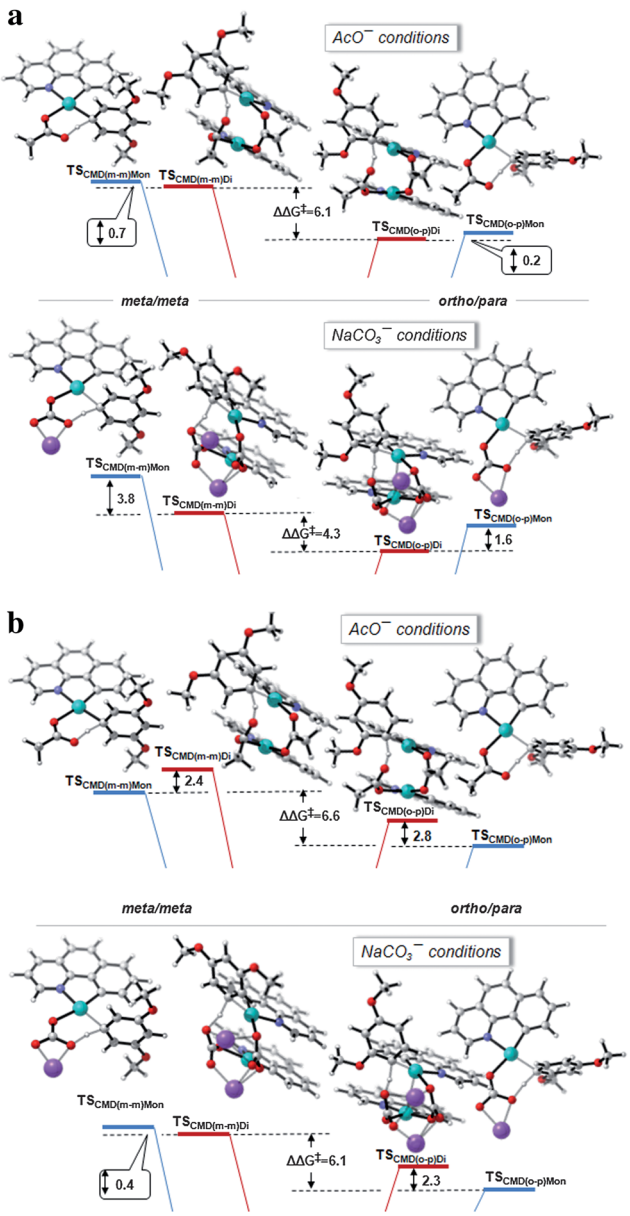

Fig. 1 (a) CMD is the favored C–H activation mechanism. Selectivity ($\Delta\Delta G^‡$) for CMD-C–H activation for acetate (top) and $NaCO_3^-$ (bottom), derived from dinuclear (Di, red) and mononuclear Pd-complexes (Mon, blue);[25] calculated at COSMO-RS (DMSO/DMB[26] = 50/300) M06L/6-31++G(d,p) (SDD for Pd)//ωB97X/6-31G(d,p) (with LANL2DZ for Pd & Na), including standard state conversion.[29] Free energies in kcal mol^{-1}. (b) Selectivity ($\Delta\Delta G^‡$) for CMD-C–H activation for acetate (top) and $NaCO_3^-$ (bottom), derived from dinuclear (Di, red) and mononuclear Pd-complexes (Mon, blue);[25] calculated at COSMO-RS (DMSO/DMB[26] = 50/300) M06L/def2-TZVPP//ωB97X/6-31G(d,p) (with LANL2DZ for Pd & Na), including standard state conversion.[29] Free energies in kcal mol^{-1}.

Fig. 1a and b illustrate the relative activation barriers and selectivities ($\Delta\Delta G^{\ddagger}$) for the CMD C–H activation transition states to generate the *ortho*/*para* (right) or *meta*–*meta* isomer (left) with AcO^- (top) and $NaCO_3^-$ (bottom) as the anion, calculated at M06L/6-31++G(d,p) (Fig. 1a) and M06L/def2-TZVPP (Fig. 1b) levels of theory with COSMO-RS solvation (for DMSO/DMB[26]).[24] In the case of the M06L/6-31++G(d,p) basis set, the monometallic and bimetallic pathways are essentially *iso*-energetic for acetate, but the dimeric pathway is favored for carbonate (Fig. 1a).[25] For def2-TZVPP basis set (see Fig. 1b), the C–H activation by a monomeric Pd(II) complex is mostly preferred for carbonate and acetate ligands. Based on our calculations, C–H activation at the *ortho* position [$\mathbf{TS_{CMD(o-p)}}$] is favored over *meta* [$\mathbf{TS_{CMD(m-m)}}$] by $\Delta\Delta G^{\ddagger} \approx 4$–7 kcal mol^{-1}. This preference is independent of the nature of the anionic ligand (AcO^- *versus* $NaCO_3^-$) and nuclearity of Pd-complexes.

We next turned our studies to the Heck type mechanism (c, Scheme 3). In previous studies by Yu and co-workers, a change in mechanism from CMD to Heck upon ligand-alteration has been claimed for the C–H activation.[3j] The Heck-type pathway involves a four-membered transition structure as illustrated in Scheme 3.[1,22,27] In analogy to the CMD mechanism above, for each anion, the two alternative isomeric transition states were calculated. We found that the predicted activation free energy barriers are considerably higher for the Heck type pathway ($\Delta\Delta G^{\ddagger} > 20$ kcal mol^{-1}), suggesting that it is not in competition with the CMD mechanism. This indicates that a change in mechanism as the origin of selectivity for acetate *versus* carbonate is highly unlikely.

Overall, these studies indicate that the favored C–H activation pathway proceeds *via* a CMD mechanism with *ortho*/*para* selectivity. This matches the selectivity obtained experimentally under carbonate conditions, but does not match that seen with acetate. We next assessed the subsequent reductive elimination step for further insight into the origin of site-selectivity.

Study of steps 2/3: reductive elimination as a function of anionic ligand and coordination sphere. The precise structural features of the reductive elimination step are currently unknown. As indicated in Scheme 2, benzoquinone coordination is believed to occur, but the geometry of the resultant complex is unknown. Moreover, it is not clear whether coordination of the ligand (L = conjugate acid of anionic ligand) occurs during the reductive elimination. Another unknown is whether the reductive elimination takes place *via* a mono- or bimetallic pathway. We initially considered a *mononuclear pathway* and studied the reductive elimination from Pd complexes containing a variety of ligands, involving (i) benzoquinone coordination, (ii) benzoquinone-free reductive elimination with only L, or (iii) reductive elimination from a complex containing neither benzoquinone nor L as ligands. Fig. 2 gives the free energy profiles for the *ortho*/*para*-pathways (B-selectivity) for the two anionic ligands, AcO^- (top) or $NaCO_3^-$ (bottom), and takes into account various coordination possibilities. The corresponding figure for the *meta*–*meta* pathways (A-selectivity) is given in the ESI (Fig. S2, page S4†). The latter shows analogous activation free energy barriers in

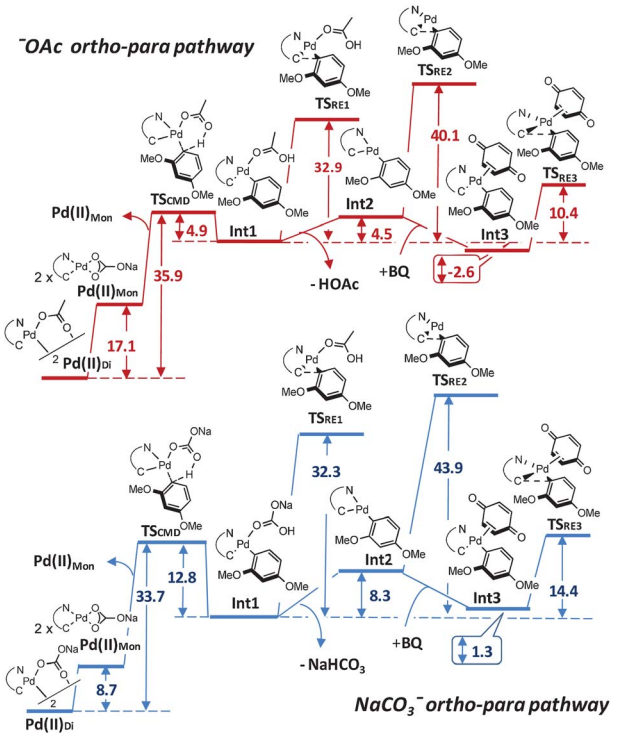

Fig. 2 Free energy profile (in kcal mol^{-1}) for acetate (top) or sodium carbonate (bottom) as anionic ligands. The *ortho*/*para*-pathway (mononuclear) was calculated and various coordination possibilities considered. Calculated at COSMO-RS (DMSO/DMB = 50/300) M06L/6-31++G(d,p) (SDD for Pd & Na)//ωB97X/6-31G(d,p) (LANL2DZ for Pd & Na), including standard state conversion.[29]

the reductive elimination with respect to the various possible coordination states.

Our calculations show that reductive elimination in the absence of benzoquinone has a prohibitively high barrier of $\Delta G^{\ddagger} > 30$ kcal mol^{-1} (see Fig. 2, $\mathbf{TS_{RE1}}$ and $\mathbf{TS_{RE2}}$). Coordination of BQ to the bis-aryl Pd center significantly decreases the barrier for reductive elimination to roughly $\Delta G^{\ddagger} \approx 13$–15 kcal mol^{-1}, *i.e.* $\mathbf{TS_{RE3}}$. The lowest energy pathway examined is therefore the one involving dissociation of the acid from **Int1**, $NaHCO_3$ respectively, followed by reductive elimination *via* the benzoquinone-coordinated $\mathbf{TS_{RE3}}$.[28]

Although the reaction is difficult to achieve, requiring the reactant in large excess (as co-solvent) and 150 °C reaction temperature over prolonged time, the calculated activation free energy barriers are still overall rather high. For the carbonate pathway we calculate an overall activation free energy barrier of $\Delta G^{\ddagger} = 35.3$ kcal mol^{-1} to reach $\mathbf{TS_{RE3}}$ (see Fig. 2); for acetate the barrier is even higher: $\Delta G^{\ddagger} = 41.4$ kcal mol^{-1}. This seems to be a consequence primarily of dispersion that stabilizes the cyclopalladated Pd(II) acetate starting complex strongly.[30,31] While dispersion is arguably crucial in the system considered (π–π interaction in Pd-dimer, Pd···BQ interaction in reductive elimination) the current methodology might overestimate these effects.[30,31]

To also assess the likelihood of bimetallic, rather than monometallic, reductive elimination, we calculated TS geometries analogous to $\mathbf{TS_{RE3}}$ from a dinuclear Pd(II). Fig. 3 compares

the free energies of the bimetallic ($\mathbf{TS_{RE3\text{-}Di}}$) and monometallic ($\mathbf{TS_{RE3\text{-}Mon}}$) reductive elimination transition states. The mononuclear pathway was found to be favored for both anionic ligands (see Fig. 3). Based on our calculations, the ligand (L) dissociates from the mononuclear complex prior to reductive elimination and the TS containing benzoquinone favors the *meta–meta* product **A** under all conditions tested.

Summary of mechanistic findings. The available data suggest that with both anionic ligands the lowest energy pathway for C–H activation involves a CMD mechanism. The calculations also indicate that the inherent selectivity of C–H activation does not change upon moving from acetate to carbonate (Fig. 1). With both of these anionic ligands, C–H activation to form the *ortho*/*para* isomer is favored. This preference holds, independent of whether C–H activation occurs at a mononuclear or dinuclear Pd(II) species. Our calculations further show that the BQ-promoted reductive elimination step favors the *meta–meta* isomer, for both mononuclear and dinuclear Pd-complexes with both anionic ligands.

Origin of site-selectivity. Having established the favored reaction pathways for C–H activation and reductive elimination, we can now compare the predicted selectivities for the two anionic ligands for di- and mononuclear pathways. Fig. 4a and 5a give an overview of the crucial selectivity-determining transition states considering bimetallic C–H activation, calculated with M06L/6-31++G(d,p)/SDD and the COSMO-RS solvation model for DMSO/DMB[26] (50 : 300). Fig. 4b and 5b compare the selectivities for monometallic pathways at the M06L/def2-TZVPP level of theory.

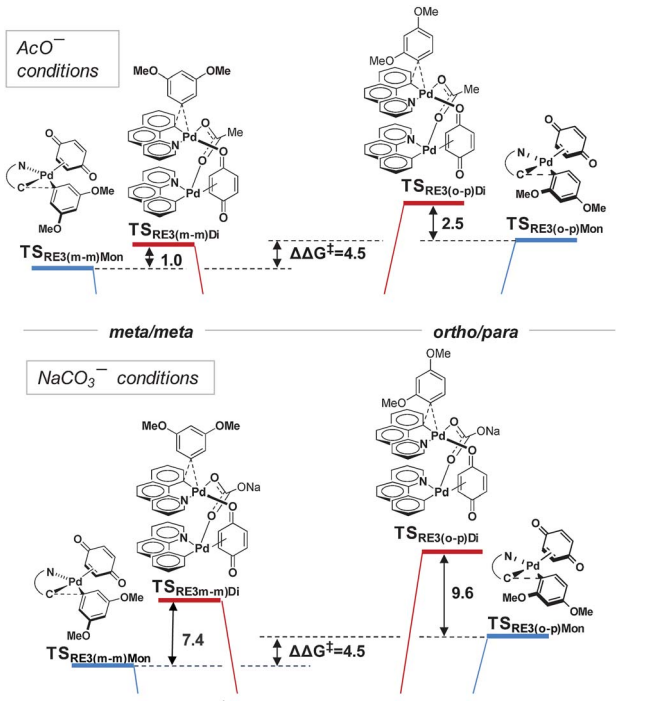

Fig. 3 Selectivity ($\Delta\Delta G^{\ddagger}$) for reductive elimination for acetate (top) and $NaCO_3^-$ (bottom), derived from dinuclear (red) and mononuclear Pd-complexes (blue); calculated at COSMO-RS (DMSO/DMB[26] = 50/300) M06L/6-31++G(d,p) (SDD for Pd & Na)//ωB97X/6-31G(d,p) (with LANL2DZ for Pd & Na), including standard state conversion.[29] Free energies in kcal mol^{-1}. The activation free energy barriers are given in Fig. 2.

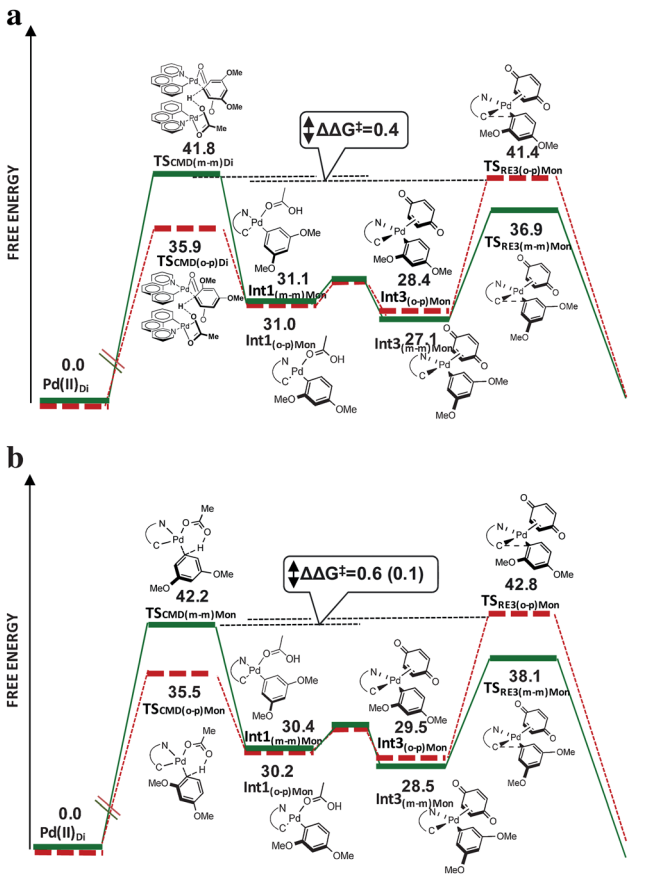

Fig. 4 (a) Overview of selectivity controlling steps for the acetate system and bimetallic C–H activation at COSMO-RS (DMSO/DMB[26] = 50 : 300) M06L/6-31++G(d,p) (SDD for Pd)//ωB97X/6-31G(d,p) (with LANL2DZ for Pd & Na). Free energies illustrated in kcal mol^{-1}.[29] (b) Overview of selectivity controlling steps for the acetate system at COSMO-RS (DMSO/DMB[26] = 50 : 300) M06L/def2-TZVPP//ωB97X/6-31G(d,p) (with LANL2DZ for Pd & Na). Free energies illustrated in kcal mol^{-1}.[29] At COSMO-RS (DMSO/DMB[26] = 50 : 300) M06L/6-31++G (d,p) (SDD for Pd), the selectivity is 1.1 kcal mol^{-1}. Energies in parenthesis are based on B3LYP geometries [COSMO-RS (DMSO/DMB[26] = 50 : 300) M06L/6-31++G(d,p) (SDD for Pd & Na)//B3LYP/6-31 + G(d) (with LANL2DZ for Pd & Na)].

When acetate acts as the ligand, (Fig. 4a and b), the C–H activation step favors the *ortho*/*para* isomer (dotted red path). However, the subsequent reductive elimination *via* $\mathbf{TS_{RE3(o-p)}}$ is close in energy to the C–H activation TS of the competing *meta–meta* pathway. Because the C–H insertion step should be reversible (based on the relative barriers for the two steps, see Fig. 4a and b), the mixture is therefore expected to partially equilibrate. The overall predicted selectivity ($\Delta\Delta G^{\ddagger}$) is small. We predicted the same small selectivity ($\Delta\Delta G^{\ddagger} \approx 1$ kcal mol^{-1}) also for alternative methods (*i.e.* PBE0-D3, see ESI, Fig. S3†). However, throughout the course of the reaction, acetic acid will be generated in the reaction mixture. With increasing acid concentration, the reverse reaction of C–H activation would be expected to be favored, making the reductive elimination the crucial selectivity-determining step (we present experimental support of these proposals in the next section).

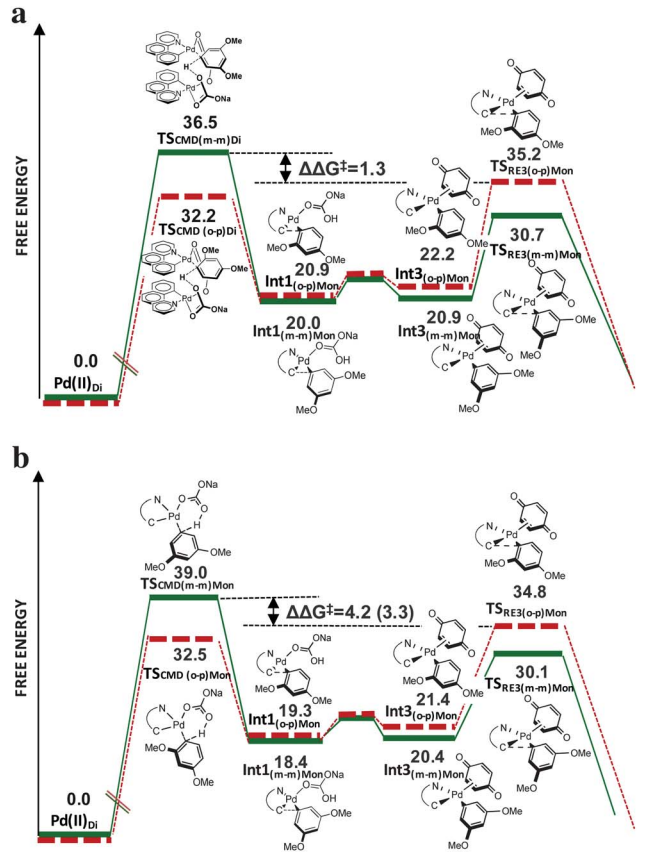

Fig. 5 (a) Overview of selectivity controlling steps for the carbonate system, considering bimetallic C–H activation; calculated at COSMO-RS (DMSO/DMB[26] = 50 : 300) M06L/6-31++G(d,p) (SDD for Pd & Na)//ωB97X/6-31G(d,p) (with LANL2DZ for Pd & Na). Free energies illustrated in kcal mol^{-1}.[29] (b) Overview of selectivity controlling steps for the carbonate system, considering monometallic pathways; calculated at COSMO-RS (DMSO/DMB[26] = 50 : 300) M06L/def2-TZVPP. Free energies illustrated in kcal mol^{-1}.[29] At COSMO-RS (DMSO/DMB[26] = 50 : 300) M06L/6-31++G (d,p) (SDD for Pd & Na), the selectivity is 5.0 kcal mol^{-1}. Energies in parenthesis are based on B3LYP geometries [COSMO-RS (DMSO/DMB[26] = 50 : 300) M06L/6-31++G(d,p) (SDD for Pd & Na)//B3LYP/6-31 + G(d) (with LANL2DZ for Pd & Na)].

For the carbonate system, the selectivity was experimentally found to be overall *ortho*/*para*-selective (see Scheme 1). Computationally, the C–H activation for the *meta*–*meta* pathway, *i.e.* $\mathbf{TS_{CMD(m-m)}}$, was found to be the highest energy TS on the free energy surface. It is therefore disfavored (see Fig. 5a and b). The *ortho*/*para* reductive elimination TS ($\mathbf{TS_{RE3(o-p)}}$) is lower in energy than the C–H activation TS for the competing *meta*–*meta*-pathway ($\mathbf{TS_{CMD(m-m)}}$) by $\Delta\Delta G^{\ddagger}$ = 1.3–4.3 kcal mol^{-1} (see Fig. 5a and b). The carbonate pathway therefore favors the *ortho*/*para* product **B**. Notably, the relative barriers for the C–H activation ($\Delta G^{\ddagger} \approx 33$ kcal mol^{-1}) and reductive elimination step ($\Delta G^{\ddagger} \approx 35$ kcal mol^{-1}) in the carbonate system are similar, which is expected to render this transformation less reversible than the analogous acetate reaction. This is also expected to contribute to the observed selectivity for **B**. Applying the alternative method PBE0-D3, the almost identical selectivity profile was obtained; (see ESI, Fig. S3 on page S4†).

In the course of the experiment, $NaHCO_3$ will be generated that could potentially participate in the reaction pathway. We tested this possibility experimentally, employing $NaHCO_3$ as the anionic ligand source in place of Na_2CO_3 under otherwise identical reaction conditions. We found that $NaHCO_3$ also gives rise to efficient conversion, and similar selectivity to that found previously with Na_2CO_3, *i.e.* the A : B ratio was 1 : 8 in favor of *ortho*/*para* product B (see page S5 in the ESI†). Thus, if $NaHCO_3$ were to coordinate to Pd(II), this would not affect the overall selectivity. These results were confirmed computationally also; see Fig. S4 on page S5 in the ESI† for the computed selectivity prediction. The calculated selectivity is in favor of *ortho*/*para*, albeit to a smaller extent than with $NaCO_3^-$. Thus, the overall selectivity that is experimentally observed under Na_2CO_3 conditions may likely arise from a mixture of Na_2CO_3 and $NaHCO_3$ derived reaction pathways.[32]

In summary, our computational data suggest that the ligand (acetate *versus* carbonate) does not induce a change of mechanism at the elementary steps, and the predicted selectivity at all steps is equivalent for carbonate and acetate. Instead, the anionic ligand controls which step of the mechanism is overall selectivity-determining.[33] For acetate, the reductive elimination step is more strongly selectivity-controlling. For carbonate, the C–H activation predominantly impacts selectivity.

Experimental investigations. If the above proposals are correct, then it should be possible to obtain greater amounts of the *ortho*/*para* product (*i.e.* the B-product) in the presence of acetate, if the reaction conditions are altered so as to render the C–H insertion step less reversible. This would disfavor equilibration and thus less *meta*–*meta* product *via* $\mathbf{TS_{CMD(m-m)}}$ (Fig. 4a and b) would be produced. In order to decrease the reversibility of the reaction, the generated "free" acetic acid would need to be removed from the reaction mixture. We hypothesized that magnesium oxide (MgO), which is commonly used to neutralize weak acids, could be used as an additional additive to the original reaction conditions for this purpose (illustrated in Scheme 1 (ref. 5)). MgO is an ideal base additive because it is insoluble, which should preclude its direct participation in the mechanism (*via* coordination and thereby serving as an anionic ligand, for example).

To our delight, upon addition of MgO, the oxidative coupling of 1,3-dimethoxybenzene with cyclopalladated benzo[*h*]quinoline in the presence of acetate as anionic ligand, showed a decrease in *meta*–*meta* selectivity (A : B = 5.0 : 1 *versus* A : B = 6.3 : 1 with no added MgO), see Fig. 6. Furthermore, when the number of equivalents of MgO was increased from 8 to 15 (thereby enhancing the efficiency of acid removal), this trend continued (A : B = 3.3 : 1, with 100% yield). These results are consistent with our computationally derived conclusions.

It was previously found that the addition of greater equivalents of BQ under the acetate conditions renders the reaction more B-selective.[5] When the equivalents of BQ were varied with increasing amounts of MgO, increasing quantities of the B-product were obtained (see Fig. 7). It should be noted that though the addition of MgO to the acetate conditions may not lead to a completely irreversible system, which should have

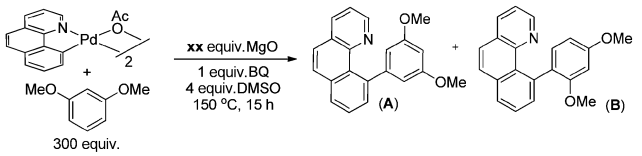

equiv.MgO	yield	ratio **A** : **B**
0 equiv.	91%	6.3 : 1
8 equiv.	100%	5.0 : 1
15 equiv.	100%	3.3 : 1

Fig. 6 Experimental tests of calculations. Enhanced B-selectivity observed in the presence of MgO under acetate conditions.

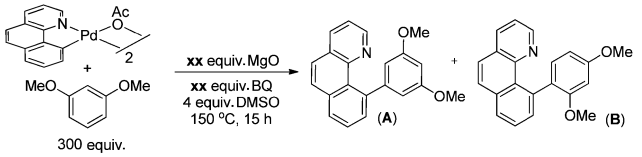

	8 equiv. MgO		15 equiv. MgO	
equiv.BQ	yield	ratio **A** : **B**	yield	ratio **A** : **B**
1 equiv.	100%	5.0 : 1	100%	3.3 : 1
3 equiv.	100%	2.5 : 1	100%	2.0 : 1
5 equiv.	100%	1.8 : 1	100%	1.3 : 1
7 equiv.	100%	1.4 : 1	100%	1.0 : 1
10 equiv.	100%	1.1 : 1	100%	0.8 : 1

Fig. 7 Experimental tests of calculations. Increased B-selectivity observed in the presence of MgO under acetate conditions.

selectivities similar to those seen under carbonate conditions, addition of more MgO does lead to more of the B-product.

Finally, we hypothesized that the addition of external acid to this system should reverse these effects, giving rise to greater *meta–meta* selectivity (A-product), since the C–H insertion would resume reversibility. We tested this scenario in Fig. 8. As predicted, the proportion of A-product increased in a dose dependent manner upon the addition of acid. This is consistent with the hypothesis that the acid moves the system back towards the original acetate system.

Conclusions

We have conducted DFT investigations to elucidate the origin of site-selectivity in the oxidative coupling of 1,3-dimethoxybenzene and benzo[*h*]quinoline as a function of anionic ligand.

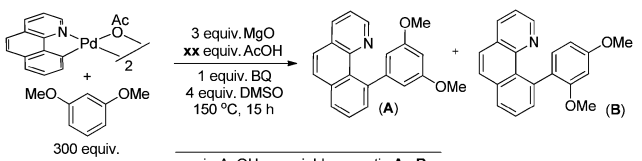

equiv.AcOH	yield	ratio **A** : **B**
0 equiv.	100%	5.8 : 1
0.5 equiv.	100%	9.7 : 1
1 equiv.	100%	12.8 : 1
3 equiv.	100%	13.2 : 1
5 equiv.	100%	14.2 : 1

Fig. 8 Experimental tests of calculations. Upon addition of external AcOH to the system with MgO, the selectivity favors product A once again.

Our data suggest that the favored C–H functionalization process involves a mononuclear C–H activation for acetate and carbonate conditions. The C–H activation involves a CMD mechanism, independent of the nature of anionic ligand (acetate *versus* carbonate) and nuclearity of the Pd-complex. The predicted selectivity is *ortho*/*para* for the C–H insertion. The reductive elimination is greatly facilitated by the coordination of benzoquinone (by $\Delta\Delta G^{\ddagger} \sim 20$ kcal mol^{-1}) and is predicted to be *meta–meta* selective. The anionic ligand (acetate *versus* carbonate) does not induce a change in mechanism at the elementary steps, and the predicted selectivity at all steps is equivalent for carbonate and acetate, regardless of whether dinuclear or mononuclear Pd complexes are considered. However, the ligand does control which step of the mechanism is overall selectivity-determining. We have tested these conclusions experimentally using a number of appropriately designed experiments. Notably, using the insoluble base MgO as an acid trap under acetate conditions (with the aim of making the C–H insertion step less reversible), gave rise to predominant *ortho*/*para* (B) selectivity in the presence of acetate.

Overall this combination of theory and experiment provides a detailed and compelling picture of the origin of site-selectivity in Pd-mediated oxidative cross-coupling. It is particularly notable that the hypotheses generated from DFT studies were confirmed through rationally designed experimental investigations. We anticipate that similar approaches will provide valuable insights into the origin of site-selectivity in a variety of other Pd-catalyzed C–H functionalization reactions.

Acknowledgements

We thank the Swiss National Science Foundation and ETH Zürich for financial support of the computational studies. The experimental studies are based upon work supported by the US Department of Energy [Office of Basic Energy Sciences] DE-FG02-08 ER 15997. AMW thanks the US National Science Foundation for a graduate fellowship. Calculations were performed on the ETH high performance cluster "Brutus".

Notes and references

1 For reviews, see: (*a*) L. Ackermann, R. Vicente and A. R. Kapdi, *Angew. Chem., Int. Ed.*, 2009, **48**, 9792; (*b*) D. Alberico, M. E. Scott and M. Lautens, *Chem. Rev.*, 2007, **107**, 174; (*c*) T. W. Lyons and M. S. Sanford, *Chem. Rev.*, 2010, **110**, 1147; (*d*) R. Giri, B.-F. Shi, K. M. Engle, N. Maugel and J.-Q. Yu, *Chem. Soc. Rev.*, 2009, **38**, 3242; (*e*) L. McMurray, F. O'Hara and M. J. Gaunt, *Chem. Soc. Rev.*, 2011, **40**, 1885.

2 S. R. Neufeldt and M. S. Sanford, *Acc. Chem. Res.*, 2012, **45**, 936.

3 (*a*) A. N. Campbell, E. B. Meyer and S. S. Stahl, *Chem. Commun.*, 2011, **47**, 10257; (*b*) M. H. Emmert, A. K. Cook, Y. J. Xie and M. S. Sanford, *Angew. Chem., Int. Ed.*, 2011, **50**, 9409; (*c*) A. J. Hickman and M. S. Sanford, *ACS Catal.*, 2011, **1**, 170; (*d*) X. Wang, D. Leow and J.-Q. Yu, *J. Am. Chem. Soc.*, 2011, **133**, 13864; (*e*) Y. Izawa and S. S. Stahl,

Adv. Synth. Catal., 2010, **352**, 3223; (*f*) Y.-H. Zhang, B.-F. Shi and J.-Q. Yu, *J. Am. Chem. Soc.*, 2009, **131**, 5072; (*g*) D. J. Schipper, L.-C. Campeau and K. Fagnou, *Tetrahedron*, 2009, **65**, 3155; (*h*) S. Potavathri, A. S. Dumas, T. A. Dwight, G. R. Naumiec, J. M. Hammann and B. DeBoef, *Tetrahedron Lett.*, 2008, **49**, 4050; (*i*) L. Eberson and L. Jönsson, *Acta Chem. Scand., Ser. B*, 1974, **28**, 771; (*j*) K. M. Engle, D.-H. Wang and J.-Q. Yu, *J. Am. Chem. Soc.*, 2010, **132**, 14137; (*k*) S. I. Gorelsky, D. Lapointe and K. Fagnou, *J. Org. Chem.*, 2012, **77**, 658; (*l*) S. L. Gorelsky, *Organometallics*, 2012, **31**, 794; (*m*) A. Petit, J. Flygare, A. T. Miller, G. Winkel and D. H. Ess, *Org. Lett.*, 2012, **14**, 3680; (*n*) E. Clot, O. Eisenstein, N. Jasim, S. A. Macgregor, J. E. McGrady and R. N. Perutz, *Acc. Chem. Res.*, 2011, **44**, 333.

4 A. R. Dick and M. S. Sanford, *Tetrahedron*, 2006, **62**, 2439.

5 (*a*) T. W. Lyons, K. L. Hull and M. S. Sanford, *J. Am. Chem. Soc.*, 2011, **133**, 4455; (*b*) K. L. Hull and M. S. Sanford, *J. Am. Chem. Soc.*, 2007, **129**, 11904; (*c*) K. L. Hull and M. S. Sanford, *J. Am. Chem. Soc.*, 2009, **131**, 9651.

6 M. J. Frisch *et al.*, *Gaussian09, Revision A.01*, for full reference, see ESI.†

7 For other examples of BQ-promoted reductive elimination, see: (*a*) J. S. Temple, M. Riediker and J. Schwartz, *J. Am. Chem. Soc.*, 1982, **104**, 1310; (*b*) J. E. Backvall, S. E. Bystrom and R. E. Nordberg, *J. Org. Chem.*, 1984, **49**, 4619; (*c*) J. E. Backvall, R. E. Nordberg and D. Wilhelm, *J. Am. Chem. Soc.*, 1985, **107**, 6892; (*d*) A. C. Albeniz, P. Espinet and B. Martin-Ruiz, *Chem.–Eur. J.*, 2001, **7**, 2481; (*e*) M. S. Chen, N. Prabagaran, N. A. Labenz and M. C. White, *J. Am. Chem. Soc.*, 2005, **127**, 6970; (*f*) X. Chen, J. J. Li, X. S. Hao, C. E. Goodhue and J. Q. Yu, *J. Am. Chem. Soc.*, 2006, **128**, 78; (*g*) M. Perez-Rodríguez, A. A. C. Braga, M. Garcia-Melchor, M. H. Perez-Temprano, J. A. Casares, G. Ujaque, A. R. deLera, R. Alvarez, F. Maseras and P. Espinet, *J. Am. Chem. Soc.*, 2009, **131**, 3650; (*h*) M. P. Lanci, M. S. Remy, W. Kaminsky, J. M. Mayer and M. S. Sanford, *J. Am. Chem. Soc.*, 2009, **131**, 15618; (*i*) G. Yin, Y. Wu and G. Liu, *J. Am. Chem. Soc.*, 2010, **132**, 11978; (*j*) A. Ishikawa, Y. Nakao, H. Sato and S. Sakaki, *Dalton Trans.*, 2010, **39**, 3279.

8 C. Sköld, J. Kleimark, A. Trejos, L. R. Odell, S. O. Nilsson Lill, P.-O. Norrby and M. Larhed, *Chem.–Eur. J.*, 2012, **18**, 4714.

9 J.-D. Chai and M. Head-Gordon, *Phys. Chem. Chem. Phys.*, 2008, **10**, 6615.

10 On the appropriateness of LANL2DZ as ECP for Pd, see: (*a*) L. E. Roy, P. J. Hay and R. L. Martin, *J. Chem. Theory Comput.*, 2008, **4**, 1029; (*b*) G. T. de Jong, M. Sola, L. Visscher and F. M. Bickelhaupt, *J. Chem. Phys.*, 2004, **121**, 9982.

11 (*a*) Y. Zhao, N. E. Schultz and D. G. Truhlar, *J. Chem. Theory Comput.*, 2006, **2**, 364; (*b*) Y. Zhao and D. G. Truhlar, *J. Chem. Phys.*, 2006, **125**, 194101; (*c*) Y. Zhao and D. G. Truhlar, *J. Phys. Chem. A*, 2006, **110**, 13126. For use of M06L in related systems: (*d*) M. C. Nielsen, E. Lyngvi and F. Schoenebeck, *J. Am. Chem. Soc.*, 2013, **135**, 1978; (*e*) A. J. Canty, A. Ariafard, M. S. Sanford and B. F. Yates, *Organometallics*, 2013, **32**, 544; (*f*) Y. Minenkov, A. Singstad, G. Occhipinti and V. R. Jensen, *Dalton Trans.*, 2012, **41**, 5526; (*g*) D. C. Powers, D. Benitez, E. Tkatchouk, W. A. Goddard, III and T. Ritter, *J. Am. Chem. Soc.*, 2010, **132**, 14092; (*h*) D. C. Powers, E. Lee, A. Ariafard, M. S. Sanford, B. F. Yates, A. J. Canty and T. Ritter, *J. Am. Chem. Soc.*, 2012, **134**, 12002.

12 On the performance of ECPs for DFT, see: (*a*) X. Xu and D. G. Truhlar, *J. Chem. Theory Comput.*, 2012, **8**, 80; (*b*) K. A. Peterson, D. Figgen, M. Dolg and H. Stoll, *J. Chem. Phys.*, 2007, **126**, 124101.

13 (*a*) The solvation contribution from COSMO-RS was calculated with COSMOtherm (F. Eckert, A. Klamt, *COSMOtherm, Version C2.1, Release 01.11*, COSMOlogic GmbH & Co. KG, Leverkusen, Germany, 2010), based on BP86/TZVP single-point energy calculation using Orca (F. Neese, ORCA, Ver. 2.9 (Rev 0), MPI for Bioinorganic Chemistry, Germany, 2011) at 298 K; (*b*) A. Klamt, F. Eckert and W. Arlt, *Annu. Rev. Chem. Biomol. Eng.*, 2010, **1**, 101.

14 (*a*) H. B. Jansen and P. Ros, *Chem. Phys. Lett.*, 1969, **3**, 140; (*b*) B. Liu and A. D. McLean, *J. Chem. Phys.*, 1973, **59**, 4557.

15 (*a*) A. D. Becke, *J. Chem. Phys.*, 1993, **98**, 5648; (*b*) C. Lee, W. Yang and R. G. Parr, *Phys. Rev. B*, 1988, **37**, 785.

16 (*a*) C. Adamo and V. Barone, *J. Chem. Phys.*, 1999, **110**, 6158; (*b*) S. Grimme, J. Antony, S. Ehrlich and H. Krieg, *J. Chem. Phys.*, 2010, **132**, 154104; (*c*) S. Grimme, *J. Comput. Chem.*, 2006, **27**, 1787. For application of DFT-D in the study of organometallic catalysis, see: (*d*) C. L. McMullin, J. Jover, J. N. Harvey and N. Fey, *Dalton Trans.*, 2010, **39**, 10833.

17 For proposals of the SEAr mechanism, see: (*a*) M. Catellani and G. P. Chiusoli, *J. Organomet. Chem.*, 1992, **425**, 151; (*b*) C. C. Hughes and D. Trauner, *Angew. Chem., Int. Ed.*, 2002, **41**, 1569; (*c*) E. J. Hennessy and S. L. Buchwald, *J. Am. Chem. Soc.*, 2003, **125**, 12084; (*d*) B. S. Lane, M. A. Brown and D. Sames, *J. Am. Chem. Soc.*, 2005, **127**, 8050.

18 (*a*) V. I. Sokolov, L. L. Troitskaya and O. A. Reutov, *J. Organomet. Chem.*, 1979, **182**, 537; (*b*) A. D. Ryabov, I. K. Sakodinskaya and A. K. Yatsimirsky, *J. Chem. Soc., Dalton Trans.*, 1985, 2629; (*c*) M. Gómez, J. Granell and M. Martinez, *Organometallics*, 1997, **16**, 2539; (*d*) M. Gómez, J. Granell and M. Martinez, *J. Chem. Soc., Dalton Trans.*, 1998, 37; (*e*) B. Biswas, M. Sugimoto and S. Sakaki, *Organometallics*, 2000, **19**, 3895; (*f*) D. L. Davies, S. M. A. Donald and S. A. Macgregor, *J. Am. Chem. Soc.*, 2005, **127**, 13754; (*g*) D. García-Cuadrado, A. A. C. Braga, F. Maseras and A. M. Echavarren, *J. Am. Chem. Soc.*, 2006, **128**, 1066; (*h*) M. Lafrance and K. Fagnou, *J. Am. Chem. Soc.*, 2006, **128**, 16496; (*i*) M. Lafrance, C. N. Rowley, T. K. Woo and K. Fagnou, *J. Am. Chem. Soc.*, 2006, **128**, 8754; (*j*) D. Garcia-Cuadrado, P. de Mendoza, A. A. C. Braga, F. Maseras and A. M. Echavarren, *J. Am. Chem. Soc.*, 2007, **129**, 6880; (*k*) S. I. Gorelsky, D. Lapointe and K. Fagnou, *J. Am. Chem. Soc.*, 2008, **130**, 10848.

19 J. Le Bras and J. Muzart, *Chem. Rev.*, 2011, **111**, 1170.

20 (*a*) D. Lapointe and K. Fagnou, *Chem. Lett.*, 2010, **39**, 1118; (*b*) Y. Boutadla, D. L. Davies, S. A. Macgregor and A. I. Poblador-Bahamonde, *Dalton Trans.*, 2009, 5820; (*c*) I. V. Seregin and V. Gevorgyan, *Chem. Soc. Rev.*, 2007, **36**, 1173; (*d*) C. J. Engelin and P. Fristrup, *Molecules*, 2011, **16**, 951; (*e*) D. Balcells, E. Clot and O. Eisenstein, *Chem. Rev.*, 2010, **110**, 749; (*f*) J. Guihaume, E. Clot, O. Eisenstein and R. N. Perutz, *Dalton Trans.*, 2010, **39**,

10510; (*g*) D. H. Ess, R. J. Nielsen, W. A. Goddard III and R. A. Periana, *J. Am. Chem. Soc.*, 2009, **131**, 11686.

21 Another alternative involving oxidative addition of the C–H bond to Pd^{II} to form a Pd^{IV} aryl hydride intermediate has previously been excluded as the mechanism. For examples, see: (*a*) Y. Boutadla, D. L. Davies, S. A. Macgregor and A. J. Poblador-Bahamonde, *Dalton Trans.*, 2009, 5820–5831; (*b*) D. G. Musaev, A. Kaledin, B. F. Shi and J. Q. Yu, *J. Am. Chem. Soc.*, 2012, **134**, 1690; (*c*) M. Albrecht, *Chem. Rev.*, 2010, **110**, 576.

22 S. Zhang, L. Shi and Y. Ding, *J. Am. Chem. Soc.*, 2011, **133**, 20218.

23 Y. Tan, F. Barrios-Landeros and J. F. Hartwig, *J. Am. Chem. Soc.*, 2012, **134**, 3683.

24 For application of DFT methods for metals, see: (*a*) G. Frenking, *Theoretical Aspects of Transition Metal Catalysis (Topics in Organometallic Chemistry)*, Springer-Verlag, Berlin Heidelberg, 2005; (*b*) T. Strassner and M. A. Taige, *J. Chem. Theory Comput.*, 2005, **1**, 848; (*c*) C. J. Cramer and D. G. Truhlar, *Phys. Chem. Chem. Phys.*, 2009, **11**, 10757; (*d*) G. T. de Jong and F. M. Bickelhaupt, *J. Chem. Theory Comput.*, 2006, **2**, 322.

25 The bimetallic pathways are also favored for carbonate and acetate if COSMO-RS (DMSO/DMB = 50/300) PBE0–D3/6-31++G(d,p)/SDD//wB97XD/6–31G(d,p) (LANL2DZ for Pd & Na) is applied. (See Fig. S1 on page S3 in the ESI†).

26 DMB = 1,3-dimethoxybenzene.

27 (*a*) S.-Y. Tang, Q.-X. Guo and Y. Fu, *Chem.–Eur. J.*, 2011, **17**, 13866; (*b*) B. Glover, K. A. Harvey, B. Liu, M. J. Sharp and M. F. Tymoschenko, *Org. Lett.*, 2003, **5**, 301.

28 Attempts to locate TSs involving acid and BQ-coordination led to dissociation of the acid in all cases.

29 The standard state was converted to 1 M in solution (+1.89 kcal mol^{-1}).

30 In this context, it has recently been found that dispersion-corrected functionals have the tendency to overestimate the binding energy of large ligands to transition metal complexes in solution, see: H. Jacobsen and L. Cavallo, *ChemPhysChem*, 2012, **13**, 562. See also: P. Rönnholm, S. O. Nilsson Lill, J. Gräfenstein, P.-O. Norrby, M. Pettersson and G. Hilmersson, *ChemPlusChem*, 2012, **77**, 799.

31 In line with this, at COSMO-RS (DMSO/DMB = 50/300) PBE0/6–31++G(d,p) (SDD for Pd)//ωB97XD/6–31G(d,p) (LANL2DZ for Pd & Na) method of theory (*i.e.* a method that accounts less well for dispersion) the barrier for C–H activation involving acetate is calculated to be lower ($\Delta G^{\ddagger}$ = 29.6 kcal mol^{-1}).

32 In line with this, our experimental selectivity analysis of the Na_2CO_3 reactions over time revealed that the selectivity was highly *ortho*/*para* selective early on in the reaction (30 : 1, after 0.5 h), but less later on (8 : 1, after 5 h). See ESI,† page S7 for further information.

33 This scenario was presented as one mechanistic possibility in our original report of this reaction (see ref. 5*a*, endnote 24). We originally disfavored it based on a few preliminary experiments. However, the computations presented herein in conjunction with the more extensive additional experiments provide strong support in its favor.